Pharm Res (2014) 31:1919–1929
DOI 10.1007/s11095-013-1293-z

RESEARCH PAPER

Predicting Nonlinear Pharmacokinetics of Omeprazole Enantiomers and Racemic Drug Using Physiologically Based Pharmacokinetic Modeling and Simulation: Application to Predict Drug/Genetic Interactions

Fang Wu • Lu Gaohua • Ping Zhao • Masoud Jamei • Shiew-Mei Huang • Edward D. Bashaw • Sue-Chih Lee

Received: 9 August 2013 / Accepted: 31 December 2013 / Published online: 4 March 2014

ABSTRACT

Purpose The objective of this study is to develop a physiologically-based pharmacokinetic (PBPK) model for each omeprazole enantiomer that accounts for nonlinear PK of the two enantiomers as well as omeprazole racemic drug.

Methods By integrating *in vitro*, *in silico* and human PK data, we first developed PBPK models for each enantiomer. Simulation of racemic omeprazole PK was accomplished by combining enantiomer models that allow mutual drug interactions to occur.

Results The established PBPK models for the first time satisfactorily predicted the nonlinear PK of esomeprazole, R-omeprazole and the racemic drug. The modeling exercises revealed that the strong time-dependent inhibition of CYP2C19 by esomeprazole greatly altered the R-omeprazole PK following administration of racemic omeprazole as in contrast to R-omeprazole given alone. When PBPK models incorporated both autoinhibition of each enantiomer and mutual interactions, the ratios between predicted and observed AUC following single and multiple dosing of omeprazole were 0.97 and 0.94, respectively.

Conclusions PBPK models of omeprazole enantiomers and racemic drug were developed. These models can be utilized to assess CYP2C19-mediated drug and genetic interaction potential for omeprazole and esomeprazole.

KEY WORDS esomeprazole · nonlinear pharmacokinetics · omeprazole · physiologically based pharmacokinetic (PBPK) model · racemic drug

ABBREVIATIONS

ADME	Absorption, distribution, metabolism and excretion
ASA	Automated sensitivity analysis
CL_{int}	Intrinsic clearance
DDI	Drug-drug interaction
EM	Extensive metabolizers
HLM	Human liver microsomes
PBPK	Physiologically based pharmacokinetic modeling
PK	Pharmacokinetics
PM	Poor metabolizers
TDI	Time-dependent inhibition
Vss	Volume of distribution at steady state
WT	Wild type

INTRODUCTION

Omeprazole, a racemic mixture of R-omeprazole and S-omeprazole (esomeprazole), is a proton pump inhibitor for the treatment of gastric acid-mediated disorders such as heart burn, gastric ulcer, and, when used in combination with antibiotics, for the eradication of H. pylori. The enantiomer esomeprazole is also available on the market. For most indications, the approved dosing regimens for omeprazole and esomeprazole are 20 mg and/or 40 mg once daily. Clinical PK studies have shown that individual enantiomers and the racemate exhibit nonlinear PK characteristics with the nonlinearity being less apparent for R-omeprazole as compared to omeprazole or esomeprazole (1). The area under the plasma concentration-time curve (AUC) increases more than dose

Electronic supplementary material The online version of this article (doi:10.1007/s11095-013-1293-z) contains supplementary material, which is available to authorized users.

F. Wu • P. Zhao • S.-M. Huang • E. D. Bashaw • S.-C. Lee (✉)
Office of Clinical Pharmacology, Office of Translational Sciences
Center for Drug Evaluation and Research, Food and Drug Administration
10903 New Hampshire Ave,
Silver Spring, Maryland 20993, USA
e-mail: suechih.lee@fda.hhs.gov

L. Gaohua • M. Jamei
SIMCYP Limited, Blades Enterprise Centre, Sheffield, UK

proportionally. When the dose is doubled from 20 mg to 40 mg following single oral doses of esomeprazole, R-omeprazole and racemic omeprazole, the AUC ratios (40 mg *vs.* 20 mg) are 2.55, 2.24 and 2.35, respectively, while the AUC ratios at steady state (40 mg QD *vs.* 20 mg QD) increase to 3.28, 2.65 and 3.55, respectively, even though there is no measurable drug concentration at 24 h postdose (1). *In vitro* studies indicated that the differential drug disposition characteristics between esomeprazole and R-omepraozole can be attributed to their differences in enzyme kinetics and enzyme inhibition potency (1–3). Although both enantiomers are metabolized by CYP2C19 and CYP3A4, the contributions of these two enzymes to metabolism of the two enantiomers were reported to differ with 73% and 27%, respectively for esomeprazole, and 98% and 2%, respectively, for R-omeprazole (4).

Besides being CYP2C19 substrates, both enantiomers are CYP2C19 inhibitors. While *in vitro* studies have shown that esomeprazole is a time-dependent inhibitor (TDI) of CYP2C19 with weak reversible inhibition potency, R-omeprazole is mainly a reversible inhibitor of CYP2C19 (3). Because both enantiomers are substrates and inhibitors of CYP2C19, the PK profile of each enantiomer is expected to differ when the racemic mixture is administered as compared to as a single agent because of mutual inhibition between the enantiomers. In addition, CYP2C19 is a polymorphic enzyme (5,6) and the consequences of the CYP2C19 polymorphism will differ for the two enantiomers. These complex factors make it difficult to delineate the PK and to predict the drug-drug interaction (DDI) potential. Using a systems biology approach such as PBPK models to integrate knowledge on absorption, distribution, metabolism and excretion (ADME) and enzyme inhibition mechanisms for the two enantiomers and subsequently for the racemic drug is necessary to predict the PK and fully understand the DDI potential.

Population compartmental pharmacokinetic models have previously been used to describe disposition data of both the individual enantiomer and racemate for other drugs (7,8). However, these models usually do not include the drug metabolic kinetics or enzyme inhibition mechanism as factors. To better predict DDI potential, there is a need to incorporate appropriate mechanisms causing the observed enantioselective PK properties into the model for the perpetrator drug. To the best of our knowledge, such a predictive model addressing metabolic and inhibition kinetics regarding racemic drugs has not been established. Because key population-related features are incorporated into the model, PBPK model can be used to evaluate drug interactions in the context of various intrinsic factors such as age, race, genetics, and organ impairment present in patients. These models can help to set up proper study designs such as dosing regimen and sampling frequency during drug discovery and drug development. PBPK modeling also has been used to support decision making in regulatory reviews (9,10).

The objective of this study was to establish PBPK models of omeprazole enantiomers by integrating the *in vitro* enzyme kinetics and CYP inhibition parameters with specific parameters derived from *in vivo* pharmacokinetic data. The models described separately the nonlinear PK properties of esomeprazole and R-omeprazole following i.v. (single dose) and oral (single dose and multiple doses) administration. The combined enantiomer models successfully predicted the PK of racemic omeprazole when taking into account the auto-inhibition and mutual inhibition of the two enantiomers. Because CYP2C19 inhibition mechanism is inherent in these models, they can be utilized to evaluate the drug exposure changes under different conditions with various extrinsic and intrinsic factors, including drug interactions and genetic polymorphism of CYP2C19.

METHODS

Data Source

Mean plasma PK profile data for esomeprazole, R-omeprazole and omeprazole following IV and oral administration at 15 mg, 20 mg, 40 mg and/or 60 mg doses were obtained from literature (1,11,12) and were digitized using GetData Digitizer (version 2, http://www.getdata-graph-digitizer.com).

Workflow in PBPK Model Construction for Omeprazole Enantiomers and the Racemate

Our PBPK model building workflow is shown in Fig. 1. We started with building a model for esomeprazole followed by another for R-omeprazole, which separately described the stereoselective disposition of each enantiomer. The models for enantiomers were then combined to further verify the individual models and to establish the model for the racemic omeprazole, which was subsequently applied to predict the omeprazole PK in CYP2C19 PMs and EMs. Unless otherwise stated, PBPK modeling and simulations were conducted using a population based PBPK software SimCYP (V.12R.2, SimCYP, Sheffield, UK).

Model Development for Esomeprazole

The schematic representation of the minimal PBPK model for describing the ADME characteristics of esomeprazole is shown in Fig. 2 (Part A). Because human PK profile exhibited an apparent one compartment distribution for esomeprazole, we selected a minimal PBPK model with four compartments, including gut, portal vein, liver and plasma compartments. The steady state volume of distribution (Vss) was 0.2 L/kg, which was estimated based on literature value (11). As an initial estimate, the hepatic intrinsic clearance (CLu_{int}) at the

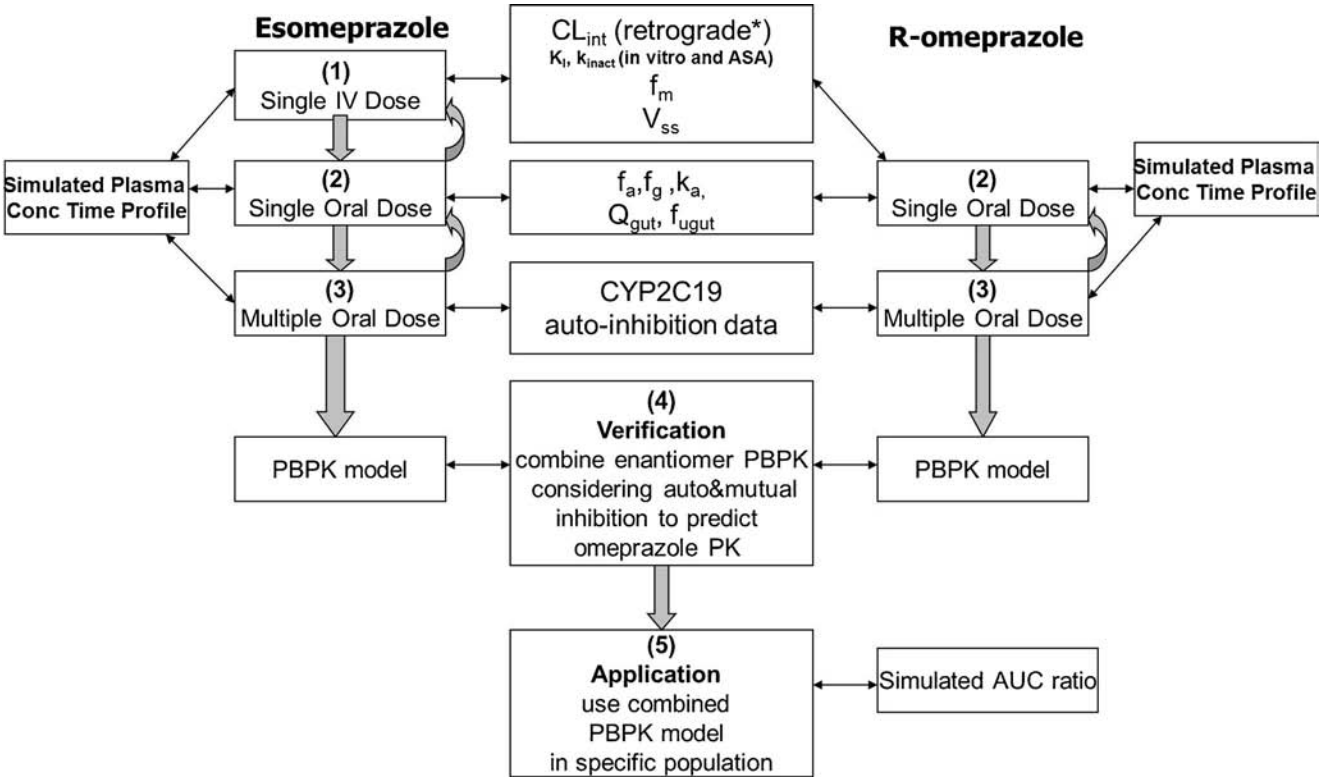

Fig. 1 Work flow for enantiomers (esomeprazole and R-omeprazole) and racemic drug (omeprazole) PBPK model building. Establishment of PBPK model by incorporating enzyme kinetics such as CL_{int} and pharmacokinetic parameters such as V_{ss} *etc.*, comparing the simulated concentration-time profile with esomeprazole or R-omeprazole PK data following (1) single IV dosing (2) single oral dosing (3) multiple oral dosing (4) verification of enantiomer model by using combined enantiomer PBPK model to predict racemic drug (omeprazole) PK. (5) application of omeprazole model. CL_{int}, *in vitro* intrinsic clearance (μL/min/pmol of isoform); K_I, concentration of inhibitor that supports half maximal inhibition (μM); k_{inact}, inactivation rate of enzyme (1/h); ASA, automated sensitivity analysis, which is a Simcyp software built-in function; fm, the relative contribution (fm) of the various elimination pathways for a drug; Vss, volume of distribution at steady state (L/kg), fa, fraction available from dosage form; fg, the fraction of drug that escapes first pass metabolism in the gut; ka, absorption rate constant (1/h); Qgut, a nominal flow in gut model(L/h); fu_{gut}, unbound fraction of drug in enterocytes; *, retrograde is a Simcyp software built-in function.

enzyme level was back-calculated from the clearance value obtained following single i.v. dosing of esomeprazole 20 mg (11) using the retrograde calculator of the software (13). Specifically, the intrinsic clearance for CYP2C19 ($CLu_{int,CYP2C19}$) and CYP3A4 ($CLu_{int,CYP3A4}$), were first estimated by accounting for the published *in vitro* findings with respect to the contribution of individual metabolic pathways ($f_{m,CYPs}$). The f_m values for CYP2C19 and CYP3A4 are 73% and 27%, respectively, for esomeprazole, and 98% and 2%, respectively, for R-omeprazole (4,12). Up to this stage, we assumed no time- or dose-dependent nonlinear PK. The first order oral absorption rate constant (ka) describing drug transfer from the gut compartment to the portal vein compartment was estimated by simultaneously fitting the pharmacokinetic data following oral administration of 20 mg or 40 mg of esomeprazole to one compartment model using Phoenix WinNonlin version 6.2 (Pharsight Co., Mountain View, CA, USA).

The above initial model for esomeprazole was coded as Model E1 (Supplementary Method 1). Model E1 was further developed by incorporating the TDI of CYP2C19 to model the nonlinear PK of esomeprazole observed *in vivo* (Supplementary Table S1). The kinetic parameters describing the TDI mechanism are the maximal inactivation rate constant (k_{inact}), the inhibitor concentration causing half-maximal inactivation (K_I) and the apparent first-order degradation rate constant for the enzyme *in vivo* (k_{deg}). The software default values of $k_{deg,CYP2C19}$ are 0.0267 and 0.03/h for the liver and gut, respectively (14). As a result of auto-inhibition of CYP2C19 (*via* TDI), $CLu_{int,organ,CYP2C19}$ value becomes time-dependent in both the gut and the liver. Note that in the initial Model E1, CLu_{int} was obtained from retrograde, which may not be the true CLu_{int}. Sensitivity analyses were conducted to explore plausible combinations of $CLu_{int,CYP2C19}$, K_I and k_{inact} of CYP2C19 for esomeprazole using human PK data from various sources. Specifically, the $CLu_{int,CYP2C19}$ at the enzyme level was fixed at three different levels (represented by modified Models E3-I, E3-II and E3-III, Supplementary Material) and a sensitivity analysis on K_I and k_{inact} was performed at each fixed level of intrinsic clearance value. The best parameter values were selected as the final model for esomeprazole (coded as Model E3-II) by comparing

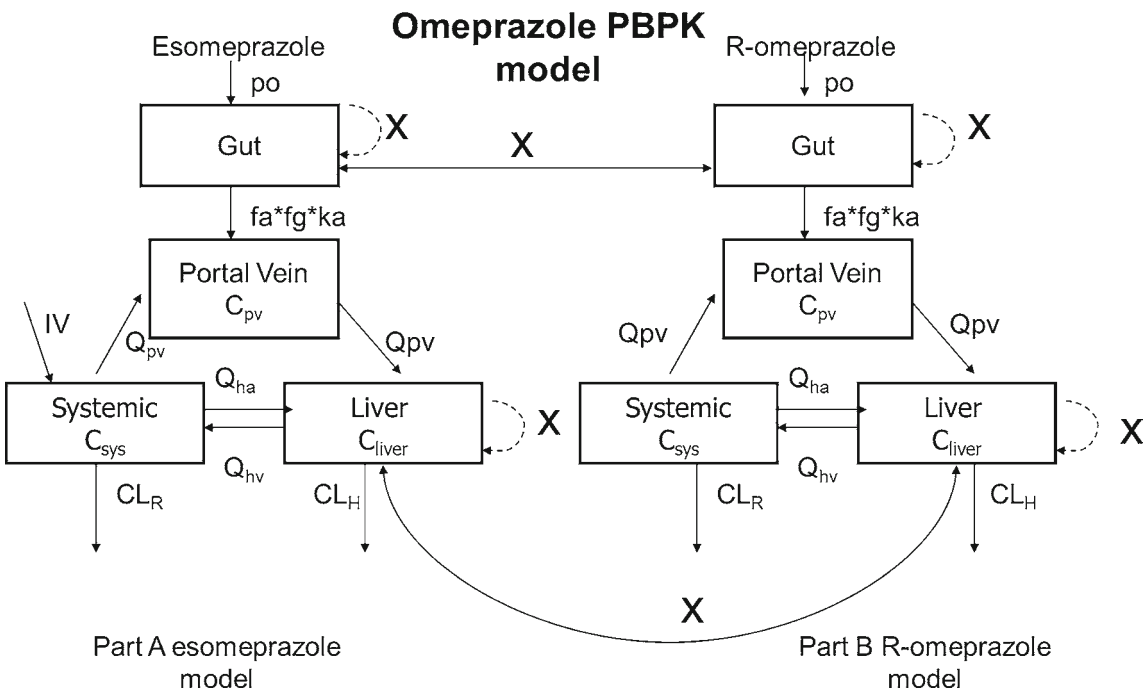

Fig. 2 The structure of Simcyp minimal PBPK model used in basic model building. X: auto- or mutual- inhibition in the gut and liver *via* time-dependent inhibition (TDI) and/or reversible inhibition of CYP2C19. Q_{pv} indicates the blood flow between portal vein and systemic compartment and between portal vein and liver. Q_{ha} and Q_{hv} indicate the blood flow between systemic compartment and liver. IV indicates the i.v. dosing to the systemic compartment. Hepatic clearance and renal clearance indicate the loss of drug from liver and kidney. po indicates oral dosing to the gut. fa indicates the fraction of drug available from dosage form. fg indicates fraction that escapes gut wall metabolism. ka indicates the absorption rate constant. C_{pv} and C_{sys} and C_{liver} are drug concentrations in the portal vein, systemic circulation and liver, respectively (μM). CL_H and CL_R are hepatic clearance and renal clearance (L/h), respectively.

the simulated PK profiles and parameters to the observed ones for IV and oral pharmacokinetic data. Details of this model modification process in determining the final parameter values for esomeprazole can be found in Supplementary Method 1. Final drug dependent parameters of esomeprazole are summarized in Table I.

Model Development for R-omeprazole

The schematic representation of the minimal PBPK model for describing the ADME characteristics of R-omeprazole is shown in Fig. 2 (Part B). The final drug dependent parameters describing the ADME processes and the inhibition mechanisms are shown in Table I. The approaches for constructing the initial model assuming no time- or dose-dependent nonlinear PK is similar to that for esomeprazole as described above, including the estimation of Ka from human plasma pharmacokinetic studies (1) using Phoenix WinNonlin. A sensitivity analysis was conducted on Vss using PK data from single oral 20 mg dose of R-omeprazole as basis for model parameter selection. The CLu_{int} values for CYP2C19 and CYP3A4 were obtained using retrograde function of SimCYP software and the *in vivo* apparent clearance for single 20 mg oral dose of R-omeprazole. In the back calculation, the value of fa*fg is taken as 1. This is because CYP2C19, the main metabolic enzyme for R-omeprazole (fm = 98%), has a low abundance in the gut (1,500 pmol *vs.* 944,000 pmol in the liver) and, thus, the gut metabolism of R-omeprazole following oral administration is expected to be negligible. The initial model for R-omeprazole (model R1) was further modified by integrating time-dependent CYP2C19 inhibition mechanism and a reversible inhibition of CYP2C19. The final model (Model R2) was selected based on sensitivity analysis of three parameter sets: $CLu_{int,\ CYP2C19}$, K_I and k_{inact} of CYP2C19 (Models R2-I, R2-II and R2-III). Details of this model modification process in determining the final parameter values for R-omeprazole can be found in Supplementary Method 2.

Construction of Omeprazole Model and Verification of R- and S-omeprazole Models

The omeprazole PBPK model was constructed by combining the models for the R- (Model R2) and S-enantiomers (Model E3-II) (Fig. 2). Specifically, one enantiomer was treated as a substrate while the other as an inhibitor in the Simcyp workspace file with each isomer representing half of the omeprazole dose. The model setup allows auto inhibition as well as mutual inhibition of CYP2C19 pathway (Table II, Model O, condition 2). Omeprazole concentrations at any specific time points were obtained by adding the simulated concentrations of two enantiomers together at the corresponding time points to generate the omeprazole PK profiles. The

Table I Drug-Dependent Parameters of Esomeprazole and R-omeprazole for the Construction of Final PBPK Model Using Simcyp (V.12R.2)

Parameters	Esomeprazole	Methods/references	R-omeprazole	Methods/references
Molecular weight	345.4	(3) [a]	345.4	(3) [a]
Log P	2.23	(3) [a]	2.23	(3) [a]
pKa	4.4, 8.7	(3) [a]	4.4, 8.7	(3) [a]
Compound type	Ampholyte	(3) [a]	Ampholyte	(3) [a]
B/P	0.59	(3) [a]	0.59	(3) [a]
fu	0.03	[b]	0.04	(3) [a]
Vss (L/kg)	0.2	(11)	0.11	Sensitivity analysis
CL_R (L/h)	0.037	(3) [a]	0.037	(3) [a]
$CLu_{int,2C19}$ (μL/min/pmol of isoform)	24.3	[c]	29.9	[d]
$CLu_{int,3A4}$ (μL/min/pmol of isoform)	0.36	[c]	0.0624	[d]
K_I CYP2C19 (μM)	0.3	[e]	1.6	[e]
k_{inact} of CYP2C19 (1/h)	5	[e]	4	[e]
fumic	1	[f]	1	[f]
fm of CYP2C19 (%)	73	(4)	98	(4)
fm of CYP3A4 (%)	27	(4)	2	(4)
ka (1/h)	10	[g]	2	[g]
fg	1	[h]	1	[h]
Qgut (L/h)	6	Predicted by Simcyp	11.4	Predicted by Simcyp
fugut	0.03	Assumed same as fup	0.04	Assumed same as fup
Ki CYP2C19 (μM)	7.5	Assume ki = IC50/2, IC50 value = 15 μM(3)	4.05	Assume ki = IC50/2, IC50 value = 8.1 μM(3)

[a] Assumed same as omeprazole, obtained from reference 3; [b] Label of esomeprazole obtained from Drugs@FDA, http://www.accessdata.fda.gov/scripts/cder/drugsatfda/; [c] Retrograde calculated value based on observed CL_{iv} (L/h) after 20 mg single dosing of esomeprazole (11); [d] Retrograde calculated value based on observed CL_{po} after 20 mg single dosing of R-omeprazole (L/h); assuming fa*fg = 1; [e] sensitivity analysis and value of omeprazole (3); [f] Simcyp compound library for omeprazole and model prediction; [g] Parameter estimated using Phoenix WinNonlin by compartmental analysis of phase I data (1); It was assumed that 100% fraction of dose can be absorbed into enterocytes from solution; [h] Gut metabolism is considered negligible

simulated omeprazole PK parameters such as AUC and Cmax were calculated using Phoenix WinNonlin and compared with the observed values. To demonstrate the contribution of mutual interaction, we also simulated PK profiles of each enantiomer given at 20 mg p.o. doses individually and added two PK profiles to generate another PK profile for 40 mg racemic omeprazole p.o. 40 mg dosing (Table II Model O without consideration of mutual inhibition, condition 1). The simulation was also performed for pharmacokinetic parameter prediction for p.o. single dosing of 20 mg racemic omeprazole.

Application of Omeprazole Model in CYP2C19 PM and EM Populations

Using healthy volunteer population in the SimCYP software, an EM population was generated by setting CYP2C19 EM frequency as 1 where the abundance of CYP2C19 in the liver for the EM population is 14 pmol/mg protein (SimCYP library). A PM population was created by setting CYP2C19 PM frequency as 1 and the abundance of CYP2C19 in the liver as 0 pmol/mg protein because *2 and *3 alleles are usually considered null alleles.

Simulations using the above omeprazole model with the consideration of mutual interactions (i.e., Model O, condition2) and esomeprazole model were performed in PM and EM populations following single oral doses of omeprazole or esomeprazole 20, 40, 60 mg in PMs and in EMs using population representatives of each phenotype. The area under the plasma concentration-time curve (AUC) and other PK parameters (Cmax, Tmax, *etc.*) were reported from Simcyp simulations. PM/EM AUC ratio for different dosing regimens of omeprazole and that for 40 mg esomeprazole were calculated and compared to the observed data (1,12,15).

RESULTS

Performance of Esomeprazole Models (Models E1, E2 and E3) for both IV and Oral Routes of Administration

Using initial esomeprazole PBPK model (Model E1, without TDI), the simulated esomeprazole profiles following single IV administration at the 20 mg and 40 mg dose levels are presented in Fig. 3a and b (dashed lines). Modified Model E3-II (final model) incorporating TDI mechanism captured the observed data reasonably well for the PK profiles following single IV dosing of esomeprazole 20 mg and 40 mg. Model E3-II, relative to Model E1, significantly improved the prediction of clearance after i.v. administration of esomeprazole 40 mg (Fig. 3a and b and Supplementary Table S1 with predicted and observed clearance values).

Table II Observed *vs.* Predicted Pharmacokinetic Parameters after Oral Single (s.d., Day 1, 0–12 h) and Multiple (m.d., Day 5, 96–120 h) Doses of 40 mg or 20 mg Omeprazole Racemic Drug and the Predicted PK Parameters of its Two Enantiomers, 20 mg or 10 mg of Esomeprazole or R-omeprazole, Using Population Representatives of the "Healthy Volunteer" Population in SimCYP

PK parameters	Drug (Dose)	Observed[a]		Predicted			
				Model O (condition 1)[b] without consideration of mutual interaction between R- and S-omeprazole while considering auto inhibition		Model O (condition 2)[c] with the consideration of auto inhibition and mutual interaction between R- and S-omeprazole	
		s.d. (day1)	m.d. (day5)	s.d. (day1)	m.d. (day5)	s.d. (day1)	m.d. (day5)
AUC[d] (μM*h)	Omeprazole (40 mg)	3.05	7.38	2.44	3.92	2.97	6.92
	Esomeprazole (20 mg)	–	–	1.63	3.02	1.73	3.65
	R-omeprazole (20 mg)	–	–	0.84	0.92	1.25	3.27
AUC[d] (μM*h)	Omeprazole (20 mg)	1.04	1.63	1.13	1.39	1.23	1.81
	Esomeprazole (10 mg)	–	–	0.72	0.97	0.74	1.05
	R-omeprazole (10 mg)	–	–	0.41	0.43	0.50	0.76

[a] Observed values from Hassen-Alin *et al.*, 2005

[b] Omeprazole concentration was obtained by adding predicted R- and S-omeprazole concentrations using separate R- and S-omeprazole PBPK models

[c] Omeprazole concentration was obtained by adding predicted R- and S-omeprazole concentration together using combined R- and S-omeprazole PBPK models (R-omeprazole as a substrate and S-omeprazole as an inhibitor or vise versa)

[d] Predicted AUC was obtained by NCA assay using Phoenix WinNonlin

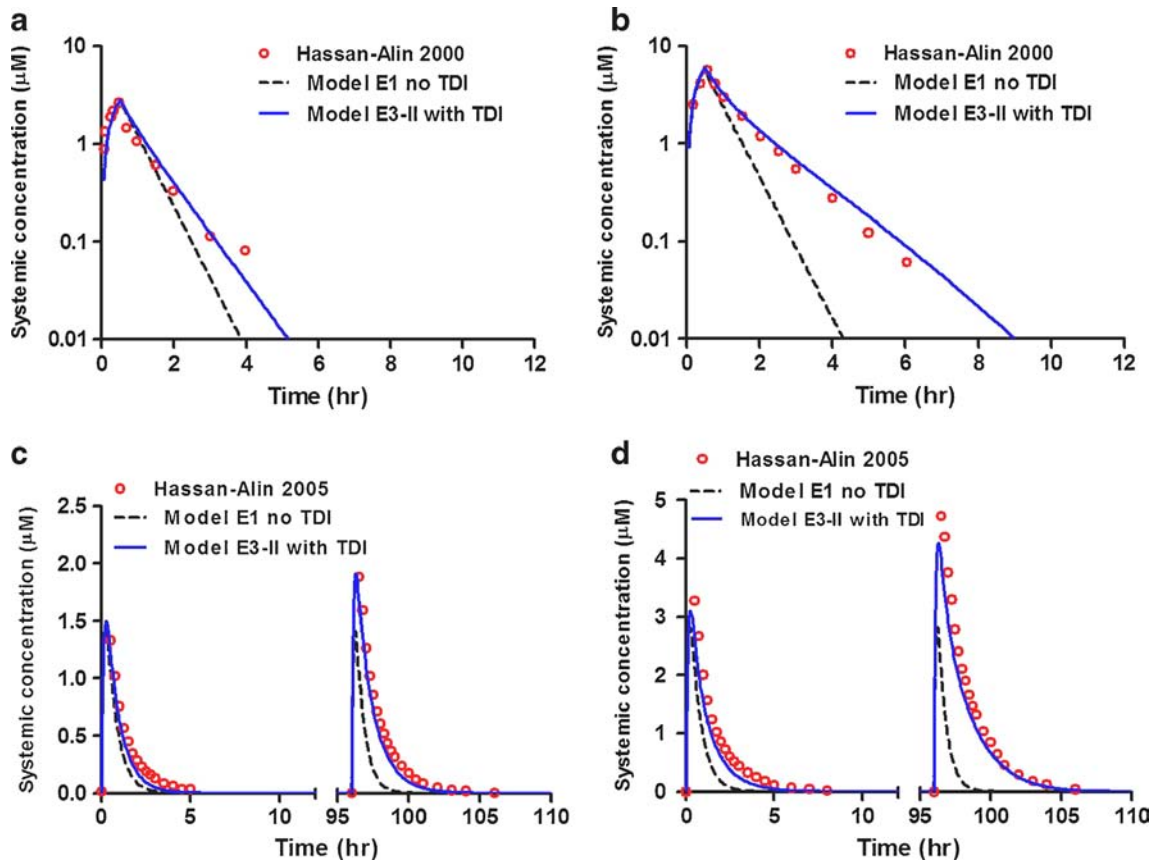

Fig. 3 Simulated (*lines*) and observed (*circles*) mean plasma concentration-time profile of esomeprazole using initial model without TDI (model E1) and modified model with TDI (model E3-II) after i.v. infusion (20 mg for 0.5 h) (**a**) and after i.v. infusion (40 mg for 0.5 h) (**b**) in healthy population representative. Simulated (*lines*) and observed (*circles*) pharmacokinetic profile at day 1 and day 5 after multiple oral administration of 20 mg q.d. dosing (**c**) and 40 mg q.d. dosing (**d**) in healthy population representative.

The performance of Model E3-II in predicting the esomeprazole PK profile following oral administration was visually compared with the PK data observed in healthy subjects. The simulated PK profiles using Model E3-II incorporating TDI described the clinical data following single (day 1) and multiple 20 mg and 40 mg q.d. dosing reasonably well (day 5) when compared with Model E1 without incorporating TDI (Fig. 3c and d). A comparison of observed and predicted PK parameters such as AUC, C_{max} and CL after single and multiple 15, 20 and 40 mg q.d. dosing of esomeprazole are given in Supplementary Table S2. Model E1 prediction of exposure *vs.* dose parallels the linear dose dependency, whereas Model E3-II is able to capture the nonlinear pharmacokinetics of esomeprazole with a time- as well as dose-dependent clearance. To evaluate the impact of the TDI parameters (K_I and k_{inact}) of CYP2C19 pathway on esomeprazole CL/F (Dose/AUC), sensitivity analysis was performed using Model E3-II as shown in Supplementary Table S2. Representative result for the impact of K_I and k_{inact} on the simulated CL/F for esomeprazole after multiple dosing (40 mg q.d.) for 5 days was shown in Supplementary Results and Supplementary Figure S1.

Performance of R-omeprazole Model

R-omeprazole concentration-time profiles following single and multiple oral doses of R-omeprazole 20 mg and 40 mg, respectively, were simulated using the initial model (Model R1) and the model incorporating time dependent inhibition mechanisms (Model R2). The pharmacokinetic parameters of R-omeprazole as estimated from simulated profiles are given in Supplementary Table S3, in comparison with those obtained from observed profiles (1, 12). These results showed that improvement in model predictions using Model R2 was more apparent following multiple dosing to address the nonlinearity characteristics, even though Model R1 can predict single dose PK well.

Verification of S- and R-omeprazole Models by Predicting Pharmacokinetics of Omeprazole

To verify the developed S- and R-omeprazole models, we predicted PK profile of omeprazole in healthy subjects following oral administration of racemic omeprazole 40 mg. By allowing both the CYP2C19 mediated auto-inhibition and mutual interactions (Model O, condition 2), the simulated AUC values of each enantiomer as well as omeprazole (i.e., the sum of esomeprazole and R-omeprazole) were generated (Table II). The simulated omeprazole AUC values were 2.97 μM·h and 6.92 μM·h on day 1 and day 5, respectively, which are comparable to those observed in healthy subjects (3.05 and 7.38 μM·h on day 1 and day 5, respectively) (1). Additionally, to demonstrate the importance of considering mutual inhibition between the two isomers, we simulated PK profiles of individual isomers following oral administration of racemic omeprazole 40 mg once daily for 5 days by including in the overall model autoinhibition for each enantiomer but not the mutual inhibition (condition 1). The calculated AUC values of omeprazole (2.44 μM·h and 3.92 μM·h on day 1 and day 5, respectively) were underestimated, especially on day 5. At the 20 mg omeprazole dose, the same trend is observed but to a lesser degree (Table II).

Exploratory Application of Racemic Omeprazole and Esomeprazole Models in CYP2C19 PM and EM Populations

The established esomeprazole and R-omeprazole models were used to simulate PK profiles following oral administration of omeprazole and esomeprazole in CYP2C19 PM and EM populations (See Methods). The predicted AUC ratio between PMs and EMs after single dosing of omeprazole 40 mg was 16.5 while the observed values ranged from 6.0 to 9.0 (15,16) (Table III). The predicted AUC ratio (PM/EM) after single dosing of esomeprazole 40 mg was 4.7, and the observed value was 3.0 (15) (Table III). In addition, the simulated PM/EM AUC ratios for omeprazole following single oral dose of omeprazole 20 mg and 60 mg were 19.9 and 13.7, respectively, while those for the esomeprazole component were 6.5 and 3.7, respectively.

DISCUSSION

Many chiral drugs are used clinically as a racemic mixture. Enantiomers of a chiral drug may differ in absorption (8), disposition (4), drug interaction with enzymes (3,17–19), pharmacological potency (20), and toxicity (21) because a structure-activity relationship may exist regarding the binding to enzymes, transporters, plasma proteins and receptors or DNA. For example, stereoselectivity in pharmacokinetics observed for albuterol is mainly due to the enantioselective metabolism of albuterol with an 8-fold higher intrinsic clearance for the pharmacologically active (R)-enantiomer than its inactive S-isomer (22,23). A recent publication demonstrated stereoselective metabolism and enzyme inhibition potency of tetrahydropalmatine (THP) enantiomers. While the metabolic rate of (+)-THP was 5-fold of (-)-THP in recombinant human CYP1A2 incubations, (-)-THP, but not (+)-THP, significantly inhibited the activity of CYP2D6 (17). For racemic drugs with stereoselective metabolism and inhibition potency, characterizing the pharmacokinetics of each enantiomer may be necessary to predict the drug interaction potential and/or pharmacological activity.

Omeprazole exhibits stereoselective metabolism by CYP2C19 and CYP3A4 as well as stereoselective CYP2C19 inhibition. *In vitro* studies indicate that esomeprazole has

Table III Observed *vs.* Predicted AUC and AUC Ratio (AUCR) in CYP2C19 PMs and EMs Taking Single Oral Dose of Racemic Omeprazole or Esomeprazole in "Healthy Volunteer" Population Representatives (0% of CYP2C19 Abundance in PMs)

PK parameters	Drug (Dose)	PMs		EMs	
		Observed[a]	Predicted[b]	Observed[a]	Predicted[b]
AUC (μM*h)	Omeprazole (60 mg)	30.1 (26.3–36.9, *n* = 5)	73.55	–	5.37
	Omeprazole (40 mg)	20.7 (20.2–21.3, *n* = 2)	49.04	3.47 (1.74–6.16, *n* = 4)	2.97
	Omeprazole (20 mg)	–	24.52	1.04 (0.64–1.72, *n* = 11)	1.23
	Esomeprazole (60 mg)	22.6 (21.5–24.5,*n* = 5)	30.08	–	8.13
	Esomeprazole (40 mg)	17.0 (16.8–17.3, *n* = 2)	20.05	5.59 (3.74–9.60, *n* = 4)	4.23
	Esomeprazole (20 mg)	–	10.03	1.52 (0.92–2.49, *n* = 11)	1.55
		Observed		Predicted	
AUCR (PM/EM)	Omeprazole (60 mg)	–		13.7	
	Omeprazole (40 mg)	6.0[c]–9.0[d]		16.5	
	Omeprazole (20 mg)	–		19.9	
	Esomeprazole (60 mg)	–		3.7	
	Esomeprazole (40 mg)	3.0[c]		4.7	
	Esomeprazole (20 mg)	–		6.5	

[a] Observed values. PK data after administration of 40 mg omeprazole/esomeprazole solution for CYP2C19 poor metabolizers and extensive metabolizers are from literature (12,15). While those data after administration of 60 mg omeprazole/esomeprazole in CYP2C19 poor metabolizers are from Andersson *et al.*, 2001, PK data after administration of 20 mg omeprazole/esomeprazole solution in CYP2C19 extensive metabolizers are from Hassen-Alin *et al.*, 2005. Observed AUC data are presented as geometric means with 95% confidence intervals

[b] Omeprazole and esomeprazole PK prediction in PMs and EMs used combined esomeprazole E3-II model and R-omeprazole R-2 model. Simulation used SimCYP® virtual healthy volunteers with CYP2C19 allele frequency set to 1 for EM and PM, respectively. And the abundance of CYP2C19 in the liver was set to 14 and 0 pmol/mg protein for EM and PM population, respectively

[c] This range was obtained from literature value (12,15)

[d] Uno T, Eur J Clin Pharmacol, 2007(16)

higher metabolic stability and more potent time-dependent CYP2C19 inhibition compared to its R-isomer and the racemate (24). When given alone, esomeprazole results in higher systemic exposure and exhibits more pronounced nonlinear kinetics compared to R-omeprazole given at the same dose (1). When omeprazole is administered as a racemic drug, not only is stereoselectivity in metabolism and CYP2C19 inhibition at play but also mutual inhibitions of the enantiomers. Thus, the plasma R- and S-omeprazole concentrations undergo dynamic changes, which differ from those when the enantiomers are given alone. Simply knowing the changes of exposure to omeprazole will not be sufficient for predicting drug interaction because the plasma R/S-omeprazole ratio changes with time and varies with dose. Our study demonstrates the utility of PBPK modeling and simulations as a mechanistic approach to predict the PK of omeprazole enantiomers and the racemate. Although the enantiomers and the racemate exhibit dose- and time-dependent PK, multiple models depending on dose or time are not necessary. Rather, a universal model with a unique set of parameters is developed for each enantiomer to predict the dose- and time-dependency in PK. Further, the model for the racemic omeprazole is analogous to a model of drug-drug interactions between the enantiomers. These models can also be utilized to predict the potential for drug interaction with other CYP2C19 substrates because the CYP2C19 inhibition mechanisms are inherent features of the models.

The PBPK models utilized information on stereoselective metabolism and interaction potency of the enantiomers, including *in vitro* CYP2C19 and CYP3A4 enzyme kinetics and CYP2C19 inhibition parameters, as well as *in vivo* PK data. The models for enantiomers describe the nonlinear PK properties and different disposition characteristics of esomeprazole and R-omeprazole following i.v. and oral dosing. The combined PBPK model predicts nonlinear omeprazole pharmacokinetics following oral administration of omeprazole 20 mg and 40 mg once daily for 5 days by generating the PK profiles for both enantiomers. Although no observed data are available, the model (Model O with mutual inhibition) predicts that, following oral administration of omeprazole 40 mg QD for 5 days, R-omeprazole AUC is more than 200% higher due to greater enzyme inhibition in the presence of esomeprazole while esomeprazole AUC is only 20.9% higher when compared to the respective enantiomer given alone (i.e., model O without mutual inhibition) (Table II).

Esomeprazole is a more potent time-dependent inhibitor than R-omeprazole (3). The TDI effect reduces the CYP2C19 activity leading to dose- and time-dependent nonlinearity. As shown in Fig. 3 and Supplementary Table S1 to S3, initial models (Models E1 and R1) without TDI could not capture

the PK nonlinearity of esomeprazole and R-omeprazole, and therefore we modified the models by incorporating the TDI effect, which captured the nonlinearity of both enantiomers reasonably well (Fig. 3, Supplementary Figure S3 and Supplementary Table S1 to S3).

K_I and k_{inact} are the two inhibition parameters that characterize a TDI effect. Values for these two parameters are reported in the literature for the racemic omeprazole but not for the individual enantiomers (3). Because of the lack of information for specific enantiomers and the uncertainty in general in the assessment of these parameters when there is a strong TDI, we carried out sensitivity analyses to obtain plausible combinations of $CLu_{int,CYP2C19}$, K_I and k_{inact} for the two enantiomers with the aid of available human PK data at different doses. Simulations and comparisons to observed nonlinear PK of each enantiomer allowed the selection of the best parameter set of $CLu_{int,CYP2C19}$, K_I and k_{inact} for the final models within SimCYP model framework (Model E3-II for esomeprazole and Model R2 for R-omeprazole). As proposed by Vieira *et al.* (13), this approach can be used during early drug development to predict enzyme inhibition potential when the *in vitro* TDI data is uncertain or unavailable while dose- and time-dependent PK nonlinearities are significant such as in the cases of esomeprazole and omeprazole. In addition, during the model building process, contribution to esomeprazole metabolism by CYP2C19 and CYP3A4 were taken as 73% and 27%, respectively, based on the *in vitro* data (4). However, since these values could have been influenced by time-dependent CYP2C19 inhibition under the experimental conditions, this can contribute to the uncertainties in $CLu_{int,CYP3A4}$ derived from retrograde method. Although errors in the estimate of $CLu_{int,CYP3A4}$ may not have a significant impact on the PK for EMs, the effect is magnified when the model is used to predict esomeprazole PK in CYP2C19 PMs.

For omeprazole given as a racemic drug containing 50:50 R- and S-isomers, the mutual interaction between R- and S-isomer played a very important role in the disposition of omeprazole enantiomers. Without considering mutual interaction, the simulated AUC of omeprazole at the 40 mg dose level is underpredicted by 46.9% on day 5 (Table II). Because the contribution of CYP2C19 metabolic pathway is 98% for the overall metabolism of R-omeprazole, which is strongly inhibited by esomeprazole, the AUC of R-omeprazole changed dramatically after consideration of mutual interaction. This is not the case for esomeprazole (Table II). The model with the consideration of both autoinhibition and mutual inhibition (i.e., Model O with mutual inhibition) demonstrated that the percentage of R-omeprazole in the total exposure after the administration of racemic drug increased from 42.1% on day 1 to 47.3% on day 5. Without consideration of mutual inhibition, the predicted R-omeprazole exposure would only account for 34.4% and 23.5% of the total AUC on day 1 and day5, respectively. At the 20 mg omeprazole dose, the same trend is observed but to a lesser degree. Thus, PBPK modeling for racemic drugs is important for predicting the dynamic changes in drug exposure and the contribution of each enantiomer, when the two enantiomers have differential pharmacological effect and/or enzyme inhibition potency.

Both R- and S-omeprazole are metabolized to form three major metabolites. The established PBPK model in this study did not consider the inhibition effect from these metabolites. A recently published article reported that some of the metabolites such as desmethyl-omeprazole are also time-dependent inhibitors of CYP2C19, which can contribute to the overall DDI potential (25). Because parent:metabolite ratio varies with dose and changes after multiple dosing, PBPK modeling would be an appropriate tool to capture these dynamic processes. The PBPK models developed here can be further refined by accounting for the inhibition by metabolites. Technically, such efforts require substantial input for each metabolite, including inhibition potency, elimination mechanism, quantitative turnover from the parent drug as well as the *in vivo* PK profile of metabolites. On the other hand, for the purpose of predicting the effect of CYP2C19 inhibition *in vivo* (e.g., on a CYP2C19 substrate), our model without incorporating metabolite inhibitions appears adequate as it satisfactorily captures dose- and time-dependent nonlinear PK of omeprazole. As such, based on current parameterization, the assumption that enzyme inhibition comes mainly from the parent drug is reasonable. This is also supported by literature data which reveal that the parent drug remains the most potent time-dependent inhibitor when plasma concentrations are also taken into consideration (3,25).

The established minimal PBPK models for both R- and S-omeprazole appear to overpredict the AUC after 15 mg single oral dosing and multiple dosing for 7 days. It should be noted that the 15 mg data is from a separate study (12) and therefore, different study subjects and other study factors can impact the PK data. This appears to be a universal challenge in using a single model to predict all observed data, because PK studies are often small in sample size, and inter-study differences in PK results can be relatively large depending on the drug of interest.

CYP2C19 is a polymorphic enzyme and poor metabolizers (PMs) are known to have significantly higher systemic exposure to omeprazole. In fact, many reports indicated better therapeutic efficacy in CYP2C19 PMs when PPIs, including omeprazole, was used for eradication of H. pylori (26–28). In one study, the AUC of omeprazole 20 mg in poor metabolizers (PMs) were found to be similar to the AUC of omeprazole 80 mg in extensive metabolizers (EMs) (29). Additionally, the AUC ratios of omeprazole 40 mg in EMs and PMs were found to range from 1:6.0 (12,15) to 1:9.0 (16) following single oral dose of omeprazole 40 mg, while it was 1:4.3 for single i.v. dose of omeprazole 20 mg (16). The PM/EM AUC ratios of omeprazole following oral dosing

among the CYP2C19 genotypes was greater than that following IV dosing, indicating first pass metabolism, primarily by the liver, plays an important role in the elimination of omeprazole. The large differences in metabolism and subsequent pharmacokinetic properties of drugs in PMs and EMs can present high inter-individual variability in efficacy and adverse reactions. As an example to test the utility of the developed PBPK model for omeprazole, we predicted the AUC ratio between PMs and EMs, which was 16.5 for single oral dose of omeprazole 40 mg and 4.7 for single oral dose of esomeprazole 40 mg (Table III). The predicted PM/EM ratio for esomeprazole generally agreed with that observed *in vivo* (3.0) (12,15) (Table III). However, our models appeared to over-predict PM/EM ratio for racemic omeprazole (16) (Table III). Because PMs have null activity of CYP2C19, elimination of omeprazole is almost exclusively *via* metabolism by CYP3A4. As mentioned earlier, the CLu_{int} of CYP3A4 for esomeprazole and R-omeprazole was obtained from the retrograde method based on *in vitro* fm values. The use of a fixed $f_{m,CYP3A4}$ value assumed linear enzyme kinetics in human liver microsomes (24) (Table I). When TDI of CYP2C19 is considered in the modified models, the assumption of linear kinetics becomes invalid, and $f_{m,CYP3A4}$ is no longer dose-independent for each enantiomer. In addition, retrograde method relied on *in vivo* clearance, and initial calculation also assumed linear pharmacokinetics (dose independent), which makes it challenging to quantify the inherent, true intrinsic clearance of CYP3A pathway. Further, for R-omeprazole, PK data from IV administration was not available and, therefore, oral PK data was used for back-calculation of intrinsic clearance of CYP enzymes. As such, additional assumptions had to be made, including the absence of gut metabolism. Ideally, *in vivo* clearance from IV administration should be used to perform retrograde analysis to reduce uncertainties. Therefore, it is likely that our models underestimated the $CLu_{int,CYP3A4}$ values for each enantiomers, causing an over-prediction of PM/EM AUC ratio. Despite the limitations described, our PBPK models largely captured PK nonlinearity and inherent mutual drug-drug interactions when racemic omeprazole is administered. Besides predicting the effect of genetic polymorphism, the models can be used to predict drug exposure in other specific populations such as pediatrics and hepatic impairment patients, and support optimal design of such studies (30–32). With regard to drug-drug interactions, the changes of amount of active CYP2C19 after multiple p.o. dosing of 40 mg (q.d. for 5 Days) esomeprazole and omeprazole (shown in Supplementary Figure S2) are valuable in determining CYP2C19 inhibition for victim drugs that are substrates of this enzyme.

In addition to the *in vivo* studies for model building and verification, we also conducted exploratory simulations for the reported drug interaction between omeprazole and fluconazole in the Korean population (Kang *et al.*, (33)). Because a virtual Korean population is currently not available, we simulated this drug interaction using developed omeprazole models and the fluconazole PBPK model in virtual Japanese, Chinese, and Caucasian populations, respectively (fluconazole drug model and populations models are available in the software's compound and population libraries). The results are described in detail in Supplementary Material. This simulation largely captured the inhibition effect by fluconazole, a strong CYP2C19 and a moderate CYP3A4 inhibitor. The predicted omeprazole AUC and Cmax ratios (with/without fluconazole) in Chinese and Caucasian population were comparable to the observed values in Kang's paper (Supplementary Results and Supplementary Table S4). This exercise also demonstrated the utility of the developed omeprazole model in predicting drug PK in different ethnic populations (Supplementary Table S4).

CONCLUSION

The established PBPK models predicted the dose- and time-dependent nonlinear PK of esomeprazole, R-omeprazole and the racemic drug by incorporating enzyme kinetic parameters as well as reversible and time dependent inhibition parameters. By adopting both "bottom up" and "top down" approaches, the model development process fully utilized prior *in vitro* and *in vivo* data. The auto-inhibition effect of enantiomers and mutual inhibition effect of racemic drug were well captured by the PBPK model. Because the PBPK models established here incorporate the enzyme inhibition mechanisms, the dynamic changes in the CYP2C19 function and the amount of active CYP2C19 can be predicted. As such, the model can be utilized to predict PK in specific populations and for assessing drug-drug interactions.

ACKNOWLEDGMENTS AND DISCLOSURES

The authors would like to thank Professor Amin Rostami-Hodjegan from the University of Manchester for his valuable scientific input. This project was supported by FDA's Critical Path Fellowship. This project was also supported in part by an appointment to the ORISE Research Participation Program at the Center for Drug Evaluation and Research administered by the Oak Ridge Institute for Science and Education through an agreement between the U.S. Department of Energy and CDER. The views presented in this manuscript are those of authors and do not necessarily reflect the official view of the FDA.

REFERENCES

1. Hassan-Alin M, Andersson T, Niazi M, Rohss K. A pharmacokinetic study comparing single and repeated oral doses of 20 mg and 40 mg omeprazole and its two optical isomers, S-omeprazole (esomeprazole) and R-omeprazole, in healthy subjects. Eur J Clin Pharmacol. 2005;60(11):779–84.
2. Li XQ, Weidolf L, Simonsson R, Andersson TB. Enantiomer/enantiomer interactions between the S- and R- isomers of omeprazole in human cytochrome P450 enzymes: major role of CYP2C19 and CYP3A4. J Pharmacol Exp Ther. 2005;315(2):777–87.
3. Ogilvie BW, Yerino P, Kazmi F, Buckley DB, Rostami-Hodjegan A, Paris BL, *et al.* The proton pump inhibitor, omeprazole, but not lansoprazole or pantoprazole, is a metabolism-dependent inhibitor of CYP2C19: implications for coadministration with clopidogrel. Drug Metab Dispos. 2011;39(11):2020–33.
4. Andersson T, Weidolf L. Stereoselective disposition of proton pump inhibitors. Clin Drug Investig. 2008;28(5):263–79.
5. Furuta T, Shirai N, Sugimoto M, Nakamura A, Hishida A, Ishizaki T. Influence of CYP2C19 pharmacogenetic polymorphism on proton pump inhibitor-based therapies. Drug Metab Pharmacokinet. 2005;20(3):153–67.
6. Hu XP, Xu JM, Hu YM, Mei Q, Xu XH. Effects of CYP2C19 genetic polymorphism on the pharmacokinetics and pharmacodynamics of omeprazole in Chinese people. J Clin Pharm Ther. 2007;32(5):517–24.
7. Foster DJ, Somogyi AA, White JM, Bochner F. Population pharmacokinetics of (R)-, (S)- and rac-methadone in methadone maintenance patients. Br J Clin Pharmacol. 2004;57(6):742–55.
8. Johansson CC, Gennemark P, Artursson P, Abelo A, Ashton M, Jansson-Lofmark R. Population pharmacokinetic modeling and deconvolution of enantioselective absorption of eflornithine in the rat. J Pharmacokinet Pharmacodyn. 2013;40(1):117–28.
9. Huang SM. PBPK as a tool in regulatory review. Biopharm Drug Dispos. 2012;33(2):51–2.
10. Huang SM, Rowland M. The role of physiologically based pharmacokinetic modeling in regulatory review. Clin Pharmacol Ther. 2012;91(3):542–9.
11. Hassan-Alin M, Andersson T, Bredberg E, Rohss K. Pharmacokinetics of esomeprazole after oral and intravenous administration of single and repeated doses to healthy subjects. Eur J Clin Pharmacol. 2000;56(9–10):665–70.
12. Andersson T, Hassan-Alin M, Hasselgren G, Rohss K, Weidolf L. Pharmacokinetic studies with esomeprazole, the (S)-isomer of omeprazole. Clin Pharmacokinet. 2001;40(6):411–26.
13. Vieira ML, Zhao P, Berglund EG, Reynolds KS, Zhang L, Lesko LJ, *et al.* Predicting drug interaction potential with a physiologically based pharmacokinetic model: a case study of telithromycin, a time-dependent CYP3A inhibitor. Clin Pharmacol Ther. 2012;91(4):700–8.
14. Yang J, Liao M, Shou M, Jamei M, Yeo KR, Tucker GT, *et al.* Cytochrome p450 turnover: regulation of synthesis and degradation, methods for determining rates, and implications for the prediction of drug interactions. Curr Drug Metab. 2008;9(5):384–94.
15. DRUGS@FDA, Clinical pharmacology review; http://www.accessdata.fda.gov/drugsatfda_docs/nda/2001/21154_nexium_biopharmr_p1.pdf. Last accessed July 12, 2013.
16. Uno T, Niioka T, Hayakari M, Yasui-Furukori N, Sugawara K, Tateishi T. Absolute bioavailability and metabolism of omeprazole in relation to CYP2C19 genotypes following single intravenous and oral administrations. Eur J Clin Pharmacol. 2007;63(2):143–9.
17. Sun SY, Wang YQ, Li LP, Wang L, Zeng S, Zhou H, *et al.* Stereoselective interaction between tetrahydropalmatine enantiomers and CYP enzymes in human liver microsomes. Chirality. 2013;25(1):43–7.
18. Tornio A, Niemi M, Neuvonen PJ, Backman JT. Stereoselective interaction between the CYP2C8 inhibitor gemfibrozil and racemic ibuprofen. Eur J Clin Pharmacol. 2007;63(5):463–9.
19. Sinko G, Kovarik Z, Reiner E, Simeon-Rudolf V, Stojan J. Mechanism of stereoselective interaction between butyrylcholinesterase and ethopropazine enantiomers. Biochimie. 2011;93(10):1797–807.
20. Markowitz JS, Patrick KS. Differential pharmacokinetics and pharmacodynamics of methylphenidate enantiomers: does chirality matter? J Clin Psychopharmacol. 2008;28(3 Suppl 2):S54–61.
21. Wainer IW, Granvil CP, Wang T, Batist G. Efficacy and toxicity of ifosfamide stereoisomers in an in vivo rat mammary carcinoma model. Cancer Res. 1994;54(16):4393–7.
22. Vakily M, Mehvar R, Brocks D. Stereoselective pharmacokinetics and pharmacodynamics of anti-asthma agents. Ann Pharmacother. 2002;36(4):693–701.
23. Walle T, Walle UK, Thornburg KR, Schey KL. Stereoselective sulfation of albuterol in humans. Biosynthesis of the sulfate conjugate by HEP G2 cells. Drug Metab Dispos. 1993;21(1):76–80.
24. Abelo A, Andersson TB, Antonsson M, Naudot AK, Skanberg I, Weidolf L. Stereoselective metabolism of omeprazole by human cytochrome P450 enzymes. Drug Metab Dispos. 2000;28(8):966–72.
25. Shirasaka Y, Sager JE, Lutz JD, Davis C, Isoherranen N. Inhibition of CYP2C19 and CYP3A4 by omeprazole metabolites and their contribution to drug-drug interactions. Drug Metab Dispos. 2013.
26. Furuta T, Ohashi K, Kamata T, Takashima M, Kosuge K, Kawasaki T, *et al.* Effect of genetic differences in omeprazole metabolism on cure rates for Helicobacter pylori infection and peptic ulcer. Ann Intern Med. 1998;129(12):1027–30.
27. Furuta T, Sagehashi Y, Shirai N, Sugimoto M, Nakamura A, Kodaira M, *et al.* Influence of CYP2C19 polymorphism and Helicobacter pylori genotype determined from gastric tissue samples on response to triple therapy for H pylori infection. Clin Gastroenterol Hepatol. 2005;3(6):564–73.
28. Shirai N, Furuta T, Moriyama Y, Okochi H, Kobayashi K, Takashima M, *et al.* Effects of CYP2C19 genotypic differences in the metabolism of omeprazole and rabeprazole on intragastric pH. Aliment Pharmacol Ther. 2001;15(12):1929–37.
29. Kita T, Sakaeda T, Aoyama N, Sakai T, Kawahara Y, Kasuga M, *et al.* Optimal dose of omeprazole for CYP2C19 extensive metabolizers in anti-Helicobacter pylori therapy: pharmacokinetic considerations. Biol Pharm Bull. 2002;25(7):923–7.
30. Leong R, Vieira ML, Zhao P, Mulugeta Y, Lee CS, Huang SM, *et al.* Regulatory experience with physiologically based pharmacokinetic modeling for pediatric drug trials. Clin Pharmacol Ther. 2012;91(5):926–31.
31. Grillo JA, Zhao P, Bullock J, Booth BP, Lu M, Robie-Suh K, *et al.* Utility of a physiologically-based pharmacokinetic (PBPK) modeling approach to quantitatively predict a complex drug-drug-disease interaction scenario for rivaroxaban during the drug review process: implications for clinical practice. Biopharm Drug Dispos. 2012;33(2):99–110.
32. Zhao P, Vieira ML, Grillo JA, Song P, Wu TC, Zheng JH, *et al.* Evaluation of exposure change of nonrenally eliminated drugs in patients with chronic kidney disease using physiologically based pharmacokinetic modeling and simulation. J Clin Pharmacol. 2012;52(1 Suppl):91S–108S.
33. Kang BC, Yang CQ, Cho HK, Suh OK, Shin WG. Influence of fluconazole on the pharmacokinetics of omeprazole in healthy volunteers. Biopharm Drug Dispos. 2002;23(2):77–81.